# Supplementary Information: Cavity-Catalyzed Hydrogen Transfer Dynamics in an Entangled Molecular Ensemble under Vibrational Strong Coupling

Eric W. Fischer*
*Theoretische Chemie, Institut für Chemie, Universität Potsdam, Karl-Liebknecht-Strasse 24-25, D-14476 Potsdam-Golm, Germany*

Peter Saalfrank
*Theoretische Chemie, Institut für Chemie, Universität Potsdam, Karl-Liebknecht-Strasse 24-25, D-14476 Potsdam-Golm, Germany and Institut für Physik und Astronomie, Universität Potsdam, Karl-Liebknecht-Straße 24-25, D-14476 Potsdam-Golm, Germany*

We provide supplementary information concerning (1) the derivation of the one-dimensional hydrogen transfer Hamiltonian and deviations from a reaction path Hamiltonian, (2) numerical details on quantum dynamics calculations via the (ML)MCTDH methods, (3) details on the initial state in terms of the vibro-polaritonic density of states and (4) a derivation of the photon number operator in length-gauge representation.

## I. ONE-DIMENSIONAL HYDROGEN TRANSFER REACTION HAMILTONIAN

### A. Reaction Potential and Minimum Energy Path

We derive the one-dimensional H-transfer Hamiltonian, $\hat{H}_S$ (Eq.(2) with $N = 1$ in the main text ), from a two-dimensional asymmetric H-transfer reaction Hamiltonian for thioacetylacetone (TAA) developed by Doslić *et al.*[1]. This Hamiltonian was constructed from *ab initio* electronic structure calculations and reads

$$\hat{H}_R = -\frac{\hbar^2}{2\mu_S}\frac{\partial^2}{\partial q^2} - \frac{\hbar^2}{2\mu_B}\frac{\partial^2}{\partial Q^2} + V(q,Q) \quad , \tag{I1}$$

with a (H-transfer) reaction coordinate, $q$, a (collective) "heavy" mode coordinate, $Q$, and corresponding reduced masses, $\mu_S = 1914.028\,m_e$ and $\mu_B = 8622.241\,m_e$, respectively.[1] The two-dimensional molecular potential energy surface (PES), $V(q,Q)$, is given by

$$V(q,Q) = V(q) + \frac{\mu_B\,\omega_B^2}{2}\left(Q - \lambda_S(q)\right)^2 \quad , \tag{I2}$$

with "heavy" mode frequency, $\omega_B = 0.0009728\,E_h$, and nonlinear coupling function, $\lambda_S(q) = a_S\,q^2 + b_S\,q^3$, determined by parameters, $a_S = 0.794\,a_0^{-1}$ and $b_S = -0.2688\,a_0^{-2}$. The reaction path potential is described in terms of an adiabatic potential

$$V(q) = \frac{1}{2}\left(V_+(q) - \sqrt{V_-^2(q) + 4\,K^2(q)}\right) \quad , \tag{I3}$$

where, $V_\pm(q) = V_1(q) \pm V_2(q)$, with diabatic harmonic PES, $V_i(q)$, and non-adiabatic coupling function, $K(q)$, defined as

$$V_i(q) = \frac{\mu_i\,\omega_i^2}{2}\,(q - q_{i,0})^2 + \Delta_i \quad , \tag{I4}$$

$$K(q) = k_c\,\exp\Big(-(q - q_c)^2\Big) \quad . \tag{I5}$$

The harmonic potentials resemble the R–OH ($V_1(q)$) and R–SH ($V_2(q)$) configurations in TAA with corresponding harmonic frequencies, $\omega_{\mathrm{OH}} = 0.01487\,E_h/\hbar$ and $\omega_{\mathrm{SH}} = 0.01247\,E_h/\hbar$, reduced masses, $\mu_{\mathrm{OH}} = 1728.46\,m_e$ and $\mu_{\mathrm{SH}} = 1781.32\,m_e$, relative energy shifts, $\Delta_{\mathrm{OH}} = 0.0\,E_h$ and $\Delta_{\mathrm{SH}} = 0.003583\,E_h$, as well as displacements, $q_{\mathrm{OH},0} = -0.7181\,a_0$ and $q_{\mathrm{SH},0} = 1.2094\,a_0$. The coupling function, $K(q)$, is determined by an amplitude, $k_c = 0.15582\,E_h$, and a displacement, $q_c = 0.2872\,a_0$.[1] Further, a molecular dipole function (neglecting the vector character of the dipole moment) is given in Ref.[1] as

$$\begin{aligned} d(q,Q) = d_0 + d_S(q - q_0) + d_B(Q - \lambda_S(q)) \\ + d_{SB}(q - q_0)(Q - \lambda(q)) \quad , \end{aligned} \tag{I6}$$

with parameters, $d_0 = 1.68\,ea_0$, $d_S = -0.129\,ea_0/a_0$, $d_B = 0.023\,ea_0/a_0$, $d_{SB} = 0.451\,ea_0/a_0^2$ and $q_0 = -0.59\,a_0$.

In the present work, where we focus on the ensemble character of isomerizing molecules, an effective approximate one-dimensional Hamiltonian, $\hat{H}_S$, and corresponding dipole function, $d(q)$, are constructed, which still resemble the main features of their two-dimensional counterparts. We derive the one-dimensional transfer Hamiltonian by minimizing, $V(q,Q)$, with respect to $Q$ as

$$\frac{\partial}{\partial Q}V(q,Q) = 0 \quad \Leftrightarrow \quad Q_0 = \lambda(q) \quad , \tag{I7}$$

such that the transfer potential and the dipole function

* ericwfischer.sci@posteo.de

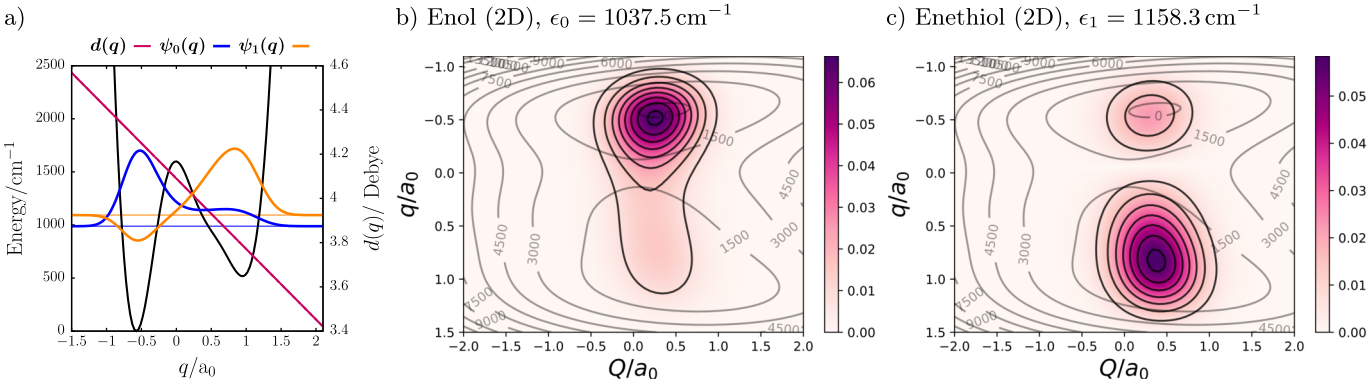


FIG. S1. (a) One-dimensional hydrogen-transfer reaction potential, $V(q)$ (in black), with dipole function, $d(q)$, and two lowest eigenstates, $\psi_0(q) = \psi_{\rm OH}(q)$ and $\psi_1(q) = \psi_{\rm SH}(q)$. (b) Ground state, $|\psi_0(q,Q)|^2 = |\psi_{\rm OH}(q,Q)|^2$, and (c) first excited state densities, $|\psi_1(q,Q)|^2 = |\psi_{\rm SH}(q,Q)|^2$, of two-dimensional reaction Hamiltonian, $\hat{H}_R$, in Eq.(I1) embedded in two-dimensional molecular PES, $V(q,Q)$, given in Eq.(I2) with contours in $\rm cm^{-1}$.

subsequently simplify to one-dimensional functions

$$V(q,Q_0) = V(q) \quad , \tag{I8}$$
$$d(q,Q_0) = d(q) = d_0 + d_S(q-q_0) \quad . \tag{I9}$$

The latter holds equivalently for an ensemble of $N$ transfer ensembles. In our study, we neglect the "heavy mode", $Q$, which does not couple *via* a potential-like term to the transfer coordinate, $q$. In Fig.S1, we show $V(q)$ and $d(q)$, with the lowest two eigenfunctions, $\psi_0(q) = \psi_{\rm OH}(q)$ (enol) and $\psi_1(q) = \psi_{\rm SH}(q)$ (enethiol), indicated. The latter were obtained by diagonalizing $\hat{H}_S$ in terms of a Colbert-Miller discrete variable representation (DVR)[5] for the transfer coordinate with $N_q = 121$ grid points and $q \in [-1.5, 2.1]\, a_0$. The corresponding eigenenergies are $\varepsilon_0 = 988.3\,\rm cm^{-1}$ and $\varepsilon_1 = 1092.8\,\rm cm^{-1}$ as stated in the main text with an energy difference of $\Delta\varepsilon_{10} = \varepsilon_1 - \varepsilon_0 = 126.5\rm cm^{-1}$.

For the two-dimensional Hamiltonian, $\hat{H}_R$, in Eq.(I1), we numerically obtain energies, $\epsilon_0 = 1037.5\,\rm cm^{-1}$ and $\epsilon_1 = 1158.3\,\rm cm^{-1}$, for the ground and first excited states, respectively, with energy difference of $\Delta\epsilon_{10} = 120.8\,\rm cm^{-1}$. Here, were we again employed a Colbert-Miller DVR with transfer grid parameters equivalent to the one-dimensional case discussed above and "heavy" mode coordinate $Q \in [-2.0, 2.0]\, a_0$ with $N_Q = 61$ grid points. Eventually, classical activation energies are by construction equivalent for the one- and two-dimensional PES with $\Delta E^{cl}_{\rm OH} = 1598\,\rm cm^{-1}$ and $\Delta E^{cl}_{\rm SH} = 1081\,\rm cm^{-1}$ as stated in the main text, since $V(q)$ is equivalent to the reaction potential along the minimum energy path on $V(q,Q)$.

### B. Deviations from a Reaction Path Hamiltonian

We discuss deviations of our approach from a reaction path Hamiltonian, which additionally involves kinetic energy couplings due to non-zero reaction path curvature. Miller, Handy and Adams[2] showed that a reaction path Hamiltonian of a two-dimensional system with mass-weighted, cartesian-like coordinates is given by

$$\hat{H}(\hat{p}_s, s, \hat{P}_s, Q_s) = \frac{\hat{p}_s^2}{2\,(1+Q_s\,\kappa(s))^2} + V_0(s) + \hat{H}_{\rm valley}(s) \quad , \tag{I10}$$

where the first two terms correspond to kinetic and potential energy contributions along the reaction coordinate, $s$, with conjugate momentum, $\hat{p}_s$, whereas the third term provides the "valley" Hamiltonian

$$\hat{H}_{\rm valley}(s) = \frac{\hat{P}_s^2}{2} + \frac{\omega(s)^2}{2}\, Q_s^2 \quad . \tag{I11}$$

The latter accounts for a $s$-dependent "valley" mode with frequency, $\omega(s)$, perpendicular to the reaction path that couples to the reaction coordinate *via* the reaction path curvature, $\kappa(s)$. For the hydrogen transfer system studied here, we have by construction, $V_0(s) = V(q,Q_0) = V(q)$.

In the following, we discuss deviations from $\hat{H}(\hat{p}_s, s, \hat{P}_s, Q_s)$, which emerge when approximating the reaction path contribution by the bare transfer Hamiltonian

$$\hat{H}_S = \frac{\hat{p}_q^2}{2} + V(q) = -\frac{\hbar^2}{2\mu_S}\frac{\partial^2}{\partial q^2} + V(q) \quad . \tag{I12}$$

This assumption is equivalent to approximately decoupling the "valley" Hamiltonian, $\hat{H}_{\rm valley}(s)$, from the reaction path contribution by assuming the reaction path curvature, $\kappa(s)$, to be small. In order to access this condition, we discuss the curvature, $\kappa(s)$, of the minimum energy or reaction path, $\underline{s}(q)$, which we introduce as parametric curve in the mass-weighted $q$-$Q$-plane[3]

$$\underline{s}(q) = (s_1(q), s_2(q))^T = (\sqrt{\mu_S}\, q, \sqrt{\mu_B}\, Q_0(q))^T \quad , \tag{I13}$$

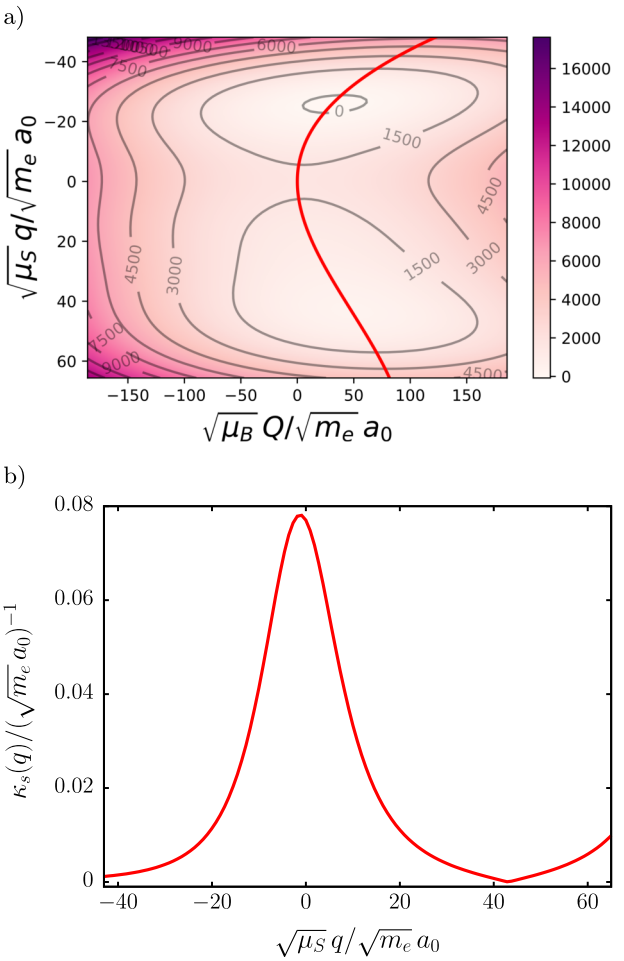


FIG. S2. a) Contour plot of molecular PES, $V(q,Q)$, in mass-weighted coordinates with reaction path, $\underline{s}(q)$, in red and colorbar in wave numbers ($\mathrm{cm}^{-1}$) and b) minimum energy path curvature, $\kappa_s(q)$, parameterized by mass-weighted transfer coordinate, $\sqrt{\mu_S}\,q$ with maximum at the transition state.

with components, $s_1(q)$ and $s_2(q)$. Here, $Q_0(q) = \lambda_S(q)$, as derived in Eq.(I7), which minimizes, $V(q,Q)$, with respect to variations in the "heavy" mode coordinate. From $\underline{s}(q)$, which is parameterized in terms of the hydrogen-transfer coordinate, $q$, we obtain the corresponding curvature, $\kappa_s(q)$, as[4]

$$\kappa_s(q) = \frac{\det\left(\underline{s}', \underline{s}''\right)}{||\underline{s}'||^3} = \frac{|s_1' s_2'' - s_1'' s_2'|}{[(s_1')^2 + (s_2')^2]^{\frac{3}{2}}} \quad , \tag{I14}$$

with derivatives, $s_i' = \frac{\partial}{\partial q} s_i(q)$ and $s_i'' = \frac{\partial^2}{\partial q^2} s_i(q)$, respectively. We like to emphasize, that $\kappa_s(q)$ depends now on the hydrogen transfer coordinate, $q$, which parametrizes the reaction path. Further, for reaction path elements, $s_1(q) = \sqrt{\mu_S}\,q$ and $s_2(q) = \sqrt{\mu_B}\,\lambda_S(q)$, we find derivatives

$$s_1' = \sqrt{\mu_S} \quad , \tag{I15}$$
$$s_2'(q) = \sqrt{\mu_B}\left(2\,a_S\,q + 3\,b_S\,q^2\right) \quad , \tag{I16}$$

and

$$s_1'' = 0 \quad , \tag{I17}$$
$$s_2''(q) = \sqrt{\mu_B}\,(2\,a_S + 6\,b_S\,q) \quad , \tag{I18}$$

which allow us to write the curvature explicitly as

$$\kappa_s(q) = \frac{2\sqrt{\mu_S\,\mu_B}\,|a_S + 3\,b_S\,q|}{\left[\mu_B\,q^2\,(2\,a_S + 3\,b_S\,q)^2 + \mu_S\right]^{\frac{3}{2}}} \quad . \tag{I19}$$

In Fig.S2a, we show the two-dimensional molecular PES, $V(q,Q)$, with reaction path, $\underline{s}(q)$, in red and the corresponding curvature, $\kappa_s(q)$, in Fig.S2b. A kinetic separation of the reaction path from the "valley" coordinate is a good approximation, if

$$\hat{T}_s = \frac{\hat{p}_s^2}{2\,(1 + Q_s\,\kappa_s(q))^2} \approx \frac{\hat{p}_q^2}{2} = \hat{T}_q \quad , \tag{I20}$$

which holds for $|Q_s\,\kappa_s(q)| \ll 1$. By taking into account the maximal curvature, $\kappa_s(q = 0.0) \approx 0.078\,(\sqrt{m_e}\,a_0)^{-1}$, at the transition state ($q = 0.0$), the coupling is solely determined by the "valley" coordinate's magnitude, which can be traced back to the excitation of the two-dimensional transfer system along the "heavy" mode. We shall estimate the latter by means of of the harmonic "valley" potential's classical turning points

$$Q_s^{\pm} = \pm\sqrt{\frac{\hbar}{\omega_B}(2v+1)} \quad , \tag{I21}$$

with vibrational quantum number, $v$, and, $\omega(q) = \omega_B$, at the transition state. For, $v = 1$, we find, $|Q_s^{\pm}\,\kappa_s(q = 0.0)| \approx 4.3$, *i.e.*, in principal already for the "heavy" mode being excited to the first excited state, which has to be expected during the transfer process, we observe a coupling to the reaction coordinate that is assumed to alter the transfer dynamics of the molecular isomerization model system. However, as the role of the "heavy" mode is *not* central for the *cavity-induced* isomerization dynamics, we consider our approximation to be qualitatively valid and sufficient to discuss entanglement-induced collective effects in the herein studied reactive vibro-polaritonic model.

## II. NUMERICAL DETAILS FOR QUANTUM DYNAMICS

We solve the TDSE (Eq.(8) in the main text) numerically by means of the multiconfigurational time-dependent Hartree (MCTDH) method and its multi-layer extension (ML-MCTDH). We propagate up to final time, $t_f = 1000\,\mathrm{fs}$, unless stated otherwise, and employ a Colbert-Miller DVR[5] for transfer reaction coordinates, $q_i \in [-1.5, 2.1]a_0$, with $N_q = 101$ grid points as well as a harmonic oscillator (HO) DVR for the cavity mode with $N_c = 101$ grid points and $x_c \in$

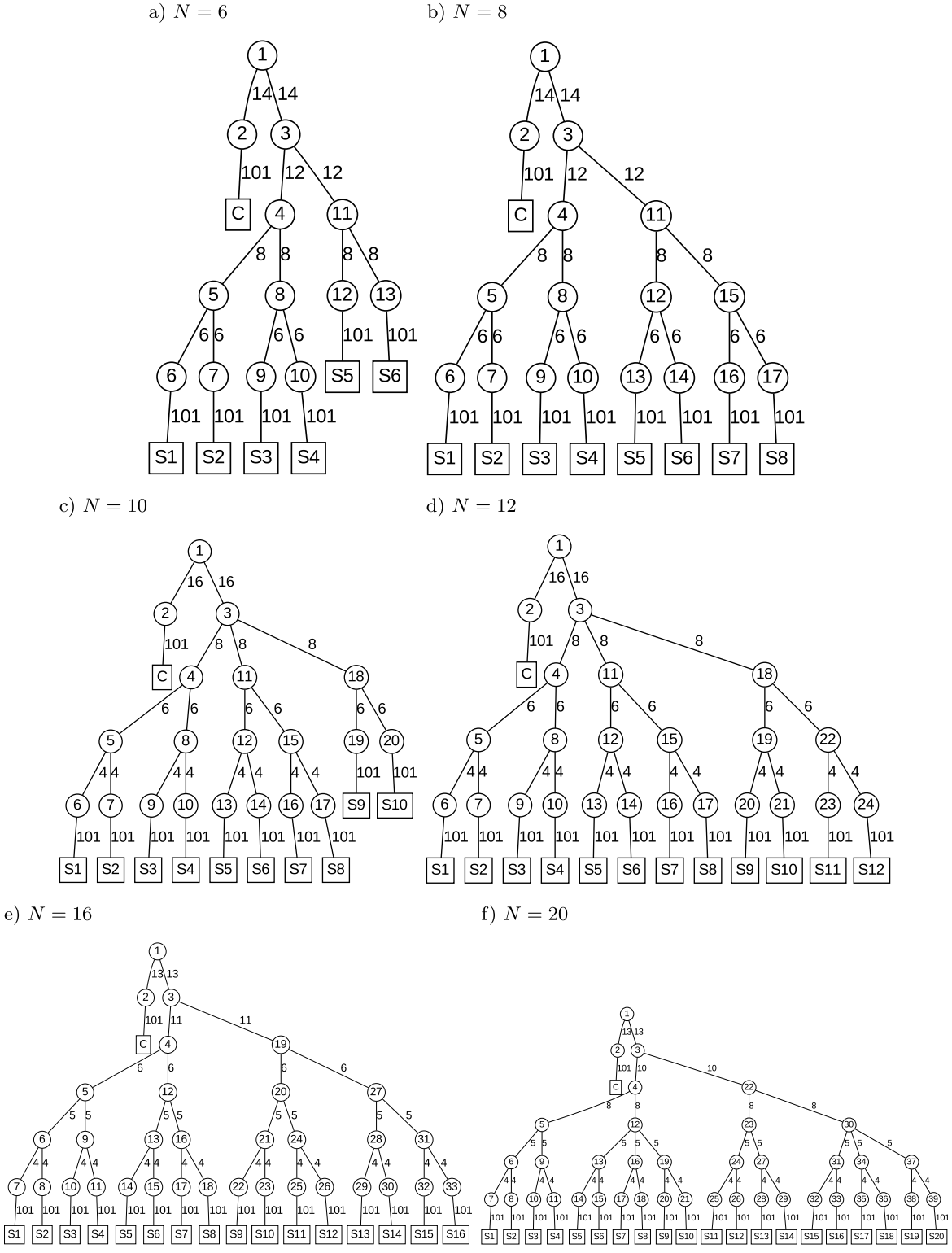


FIG. S3. Multilayer trees for different ensemble sizes $N$ with $S1$ to $SN$ transfer systems and cavity mode $C$. Number of SPFs are shown next to bonds connecting circular nodes and number of primitive basis functions are shown next to bonds connecting circular and square nodes. All trees are employed for light-matter interaction $\eta = 0.05$.

$[-561.35, +561.35]\sqrt{m_e}\, a_0$. We treat ensembles up to $N = 4$ via the MCTDH method with single particle functions (SPFs), $n_s = n_c = 10$. For ensembles with $4 < N \leq 20$, we employ the ML-MCTDH method with

converged trees (max. natural population $\leq 10^{-4}$) for all $N$ as displayed in Fig.S3. We employ the same DVR with identical number of primitive basis functions as above independent of ensemble size, $N$, but $N$-dependent numbers of SPFs, as shown next to bonds in ML trees. The latter is a result of different entanglement structure in the full vibro-polaritonic wave packet for different $N$.

## III. INITIAL STATE AND VIBRO-POLARITONIC DENSITY OF STATES

We analyze the initial state (*cf.* Eq.(9) in main text) in terms of its vibro-polaritonic contributions, which we access by means of the vibro-polaritonic density of states (DOS)

$$\sigma(\hbar\omega) = \int_0^{2t_f} C(t)\, e^{\mathrm{i}E\,t/\hbar}\mathrm{d}t \quad , \tag{III1}$$

$$= \sum_p |\,\langle\Psi_0|\Psi_p\rangle\,|^2\,\delta(E-E_p)) \quad . \tag{III2}$$

Here, $C(t) = \langle\Psi(t/2)|\Psi(t/2)\rangle$ is the autocorrelation function and, $t_f$, is the final propagation time, which we here chose as, $t_f = 3000\,\mathrm{fs}$. Further, we have vibro-polaritonic eigenenergies, $E_p$, and corresponding eigenstates, $|\Psi_p\rangle$, satisfying the time-independent Schrödinger equation

$$\left(\hat{H}_S + \hat{H}_C + \hat{H}_{SC} + \hat{H}_{DSE}\right)|\Psi_p\rangle = E_p\,|\Psi_p\rangle \quad . \tag{III3}$$

which we solve for the ground state by imaginary time evolution employing the MCTDH method. We provide an illustrative discussion for the molecular dimer, $N = 2$, interacting with the cavity mode.

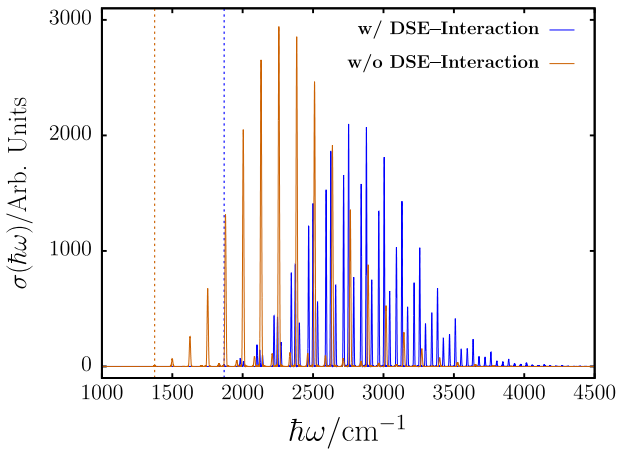


FIG. S4. Vibro-polaritonic density of states, $\sigma(\hbar\omega)$, for $N = 2$ hydrogen transfer systems strongly coupled to a single cavity mode as obtained for initial states propagated under the action of the effective Pauli-Fierz Hamiltonian with (blue) and without (orange) DSE-induced dipole-dipole interaction. Vibro-polaritonic ground state energies of $1867\,\mathrm{cm}^{-1}$ (blue) and $1374\,\mathrm{cm}^{-1}$ (orange) are indicated by dashed vertical lines.

In Fig.S4, we show $\sigma(\hbar\omega)$ for two different scenarios, where we either account for the full DSE contribution (*cf.* Eq.(6) main text) including the dipole-dipole interaction (blue graph) or where we exclude the dipole-dipole interaction and keep only the diagonal DSE contributions (orange graph). We first realize that in both cases, the envelope approximately reflects a Poisson distribution, which by recalling the cPES shift along the cavity displacement coordinate axis can be rationalized as follows: Instead of considering a shift of the cPES along the negative $x_c$-axis relative to the initial state's location, we can understand the initial state to be shifted relative to the cPES in positive $x_c$-direction instead. A shift of the cavity ground state along $x_c$ results in a coherent state, whose components in terms of cavity number states follow a Poisson distribution[6]

$$P(n_c) = e^{-\langle\hat{n}_c\rangle}\,\frac{\langle\hat{n}_c\rangle^{n_c}}{n_c!} \quad , \tag{III4}$$

with photon number, $n_c$, and length-gauge photon number expectation value, $\langle\hat{n}_c\rangle$ (*cf.* section IV below). The maximum of $P(n_c)$ is given by, $\langle\hat{n}_c\rangle$, which we found numerically for the fully interacting situation to be initially, $\langle\hat{n}_c\rangle_0 = 7.7$ (*cf.* Fig.S5 for $N = 2$). The corresponding density of states is given in Fig.S4 in blue, with the peak of maximal intensity located at $2752\,\mathrm{cm}^{-1}$ and the first peak corresponding to the vibro-polaritonic ground state located at $1867\,\mathrm{cm}^{-1}$ (indicated by a vertical, blue dashed line). The latter is solely determined by the cavity ground state with $n_c = 0$ photons. Thus, we find for the maximum intensity peak and a cavity mode energy of $\hbar\omega_c = 126.5\,\mathrm{cm}^{-1}$ approximately $n_c = 7$ photons, which agrees well with the numerically obtained $\langle\hat{n}_c\rangle_0 = 7.7$. Deviations can be traced back to the strong coupling of cavity mode and molecular systems, such that the initial state is actually not a bare coherent state in the cavity subspace but a correlated light-matter hybrid state with coherent character in the cavity mode.

We eventually address differences between blue and orange graphs in Fig.S4 due to DSE-induced dipole-dipole interactions. We observe the approximate result in orange to be red-shifted relative to the fully interacting result in blue, with ground state energy indicated by a vertical, orange dashed line. We attribute this negative energy shift to an artificial effect induced by the light-matter interaction contribution in the truncated Hamiltonian, which is compensated for when fully accounting for the DSE term[7]. Note, global energy shifts are not accessible in experiment, where only relative energies are measured and the effects of a global shift cancel. Further, when the full DSE term is included, cavity-induced dipole-dipole interactions between hydrogen transfer systems lead to the formation of additional vibro-polaritonic states. This can be interpreted as a cavity-induced *pseudo* Kasha effect, which emerges from light-matter interaction involving *transverse* cavity fields. We shall point out, that the molecular Kasha effect results from molecular dipole-dipole interactions based

on *longitudinal* electric field components (Coulomb-type interaction)[8].

## IV. PHOTON NUMBER OPERATOR IN LENGTH-GAUGE REPRESENTATION

In the main text, the expectation value of the photon number operators was used to analyze the cavity-induced H-transfer dynamics. The single-mode photon number operator, $\hat{n}_c = \hat{a}_c^\dagger \hat{a}_c$, can be written in terms of the single-mode cavity Hamiltonian, $\hat{H}_C = \hbar\omega_c \left(\hat{a}_c^\dagger \hat{a}_c + \frac{1}{2}\right)$, as

$$\hat{n}_c = \hat{a}_c^\dagger \hat{a}_c = \frac{1}{\hbar\omega_c}\hat{H}_C - \frac{1}{2} \quad , \tag{IV1}$$

where, $\hat{a}_c^\dagger$ and $\hat{a}_c$ are bosonic photon creation and annihilation operators, respectively. In length gauge representation, $\hat{n}_c$, takes the form[7, 9–11]

$$\mathcal{S}^\dagger \mathcal{U}^\dagger \, \hat{a}_c^\dagger \hat{a}_c \mathcal{U}\, \mathcal{S} = \frac{1}{\hbar\omega_c}\left(\mathcal{S}^\dagger \mathcal{U}^\dagger \, \hat{H}_C \, \mathcal{U}\, \mathcal{S}\right) - \frac{1}{2} \quad , \tag{IV2}$$

with unitary operator, $\mathcal{U} = \exp\left[\frac{\mathrm{i}}{\hbar}\hat{A}\, d(q)\right]$, mediating the Power-Zienau-Woolley (PZW) transformation as generated by the molecular dipole moment, $d(q)$, and the transverse (single-mode) vector potential, $\hat{A} = \frac{g}{\omega_c}\left(\hat{a}_c^\dagger + \hat{a}_c\right)$. A second unitary rotation mediated by, $\mathcal{S} = \exp\left[\mathrm{i}\frac{\pi}{2}\,\hat{a}_c^\dagger \hat{a}_c\right]$, acts exclusively on the cavity mode subspace and provides a real light-matter interaction term, $\hat{H}_{SC}$. Under $\mathcal{U}$ and $\mathcal{S}$, photon creation and annihilation operators transform as

$$\mathcal{S}^\dagger \mathcal{U}^\dagger \, \hat{a}_c^\dagger \mathcal{U}\, \mathcal{S} = -\mathrm{i}\, \hat{a}_c^\dagger - \frac{\mathrm{i}}{\hbar}\frac{g}{\omega_c} d(q) \quad , \tag{IV3}$$

$$\mathcal{S}^\dagger \mathcal{U}^\dagger \, \hat{a} \, \mathcal{U}\, \mathcal{S} = +\mathrm{i}\, \hat{a}_c + \frac{\mathrm{i}}{\hbar}\frac{g}{\omega_c} d(q) \quad . \tag{IV4}$$

Employing the latter identities, the transformed number operator turns with

$$\hbar\omega_c \left(\mathcal{S}^\dagger \mathcal{U}^\dagger \, \hat{a}_c^\dagger \hat{a}_c \mathcal{U}\, \mathcal{S}\right) = \hbar\omega_c \left(-\mathrm{i}\, \hat{a}_c^\dagger - \frac{\mathrm{i}}{\hbar}\frac{g}{\omega_c} d(q)\right)\left(+\mathrm{i}\, \hat{a}_c + \frac{\mathrm{i}}{\hbar}\frac{g}{\omega_c} d(q)\right) \quad , \tag{IV5}$$

$$= \hbar\omega_c \left(\hat{a}_c^\dagger \hat{a}_c + \frac{g\, d(q)}{\hbar\omega_c}\left(\hat{a}_c^\dagger + \hat{a}_c\right) + \frac{g^2}{(\hbar\omega_c)^2}\, d^2(q)\right) \quad , \tag{IV6}$$

$$= \hbar\omega_c \, \hat{a}_c^\dagger \hat{a}_c + g\, d(q)\left(\hat{a}_c^\dagger + \hat{a}_c\right) + \frac{g^2}{\hbar\omega_c}\, d^2(q) \tag{IV7}$$

as well as identities, $x_c = \sqrt{\frac{\hbar}{2\omega_c}}\left(\hat{a}_c^\dagger + \hat{a}_c\right)$, and, $\hat{p}_c = \mathrm{i}\sqrt{\frac{\hbar\omega_c}{2}}\left(\hat{a}_c^\dagger - \hat{a}_c\right)$, into

$$\mathcal{S}^\dagger \mathcal{U}^\dagger \, \hat{a}_c^\dagger \hat{a}_c \mathcal{U}\, \mathcal{S} = \frac{1}{\hbar\omega_c}\left(\underbrace{\frac{\hat{p}_c^2}{2} + \frac{\omega_c^2}{2}\, x_c^2}_{=\hat{H}_C} + \underbrace{\sqrt{\frac{2\omega_c}{\hbar}}\, g\, d(q)\, x_c}_{=\hat{H}_{SC}} + \underbrace{\frac{g^2}{\hbar\omega_c}\, d^2(q)}_{=\hat{H}_{DSE}}\right) - \frac{1}{2} \quad , \tag{IV8}$$

$$= \frac{1}{\hbar\omega_c}\left(\hat{H}_C + \hat{H}_{SC} + \hat{H}_{DSE}\right) - \frac{1}{2} \quad . \tag{IV9}$$

This latter expression enters the cavity photon number expectation value, $\langle \hat{n}_c \rangle$, in Eq.(14) of the main text. The same arguments generalize to $\hat{n}_c$ for ensembles of $N$ molecules as the unitary operator mediating the PZW transformation, $\mathcal{U}_N = \prod_i^N \mathcal{U}_i$, factorizes due the form of the ensemble dipole function, $d(q) = \sum_i^N d(q_i)$. In Fig.S5, we eventually provide the time-evolution of the bare photon number operator expectation value without normalization to the initial value.

[1] N. Doslić, K. Sundermann, L. González, O. Mó, J. Giraud-Girard, O. Kühn, *Phys. Chem. Chem. Phys.* **1**, 1249, (1999).

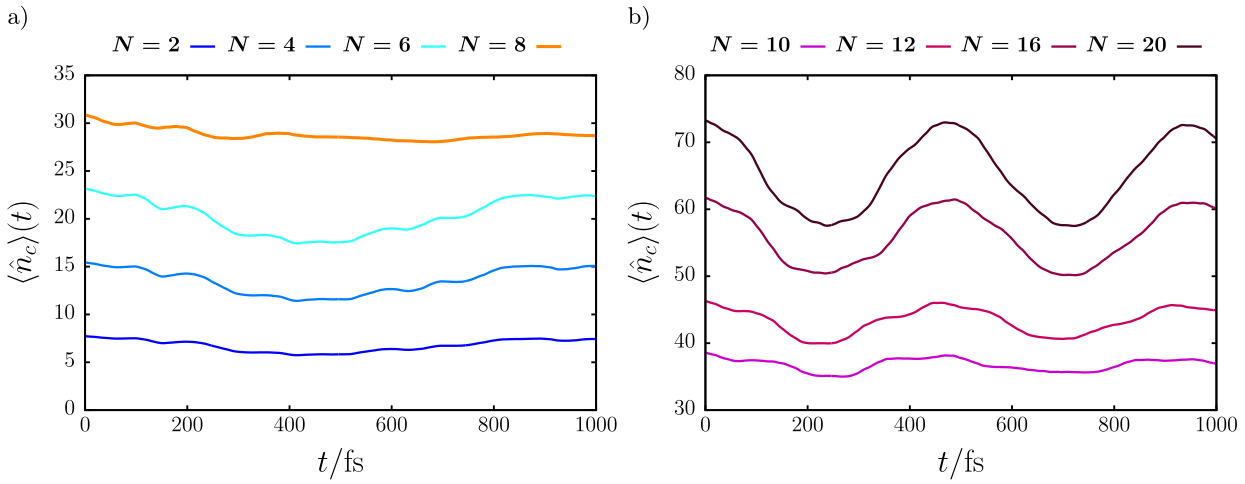


FIG. S5. Time-evolution of photon number expectation value, $\langle \hat{n}_c \rangle (t)$, as function of ensemble size $N$ for light-matter interaction strength, $\eta = 0.05$.


[2] W. H. Miller, N. C. Handy, J. E. Adams, *J. Chem. Phys.* **72**, 99, (1979).

[3] E. W. Fischer, J. Anders, P. Saalfrank, *J. Chem. Phys.* **156**, 154305, (2022).

[4] T. Arens, F. Hettlich, C. Karpfinger, U. Kockelkorn, K. Lichtenegger, H. Stachel. Mathematik. Springer Spektrum Berlin, (2018).

[5] D.T. Colbert, W.H. Miller, *J. Chem. Phys.* **96**, 1982, (1992).

[6] P. W. Milonni, *An Introduction to Quantum Optics and Quantum Fluctuations*, Oxford University Press, (2019).

[7] E. W. Fischer, P. Saalfrank, *J. Chem. Phys.* **154**, 104311 (2021).

[8] N. J. Hestand, F. C. Spano, *Chem. Rev.* 2018, 118, 7069–7163

[9] V. Rokaj, D. M. Welakuh, M. Ruggenthaler, A. Rubio, *J. Phys. B: At., Mol. Opt. Phys.* **51**, 034005 (2018).

[10] C. Schäfer, M. Ruggenthaler, V. Rokaj, A. Rubio, *ACS Photonics* **7**, 975 (2020).

[11] A. Mandal, T. D. Krauss, P. Huo, *J. Phys. Chem. B* **124**, 6321, (2020).